Electronic Supplementary Material for CrystEngComm

Supplementary Information:

Precursory disilver(I) macrocycle with pendent binding sites: a new building block for targeting coordination polymers based on solvent-controlled conformational variation

Wei Wei, Mingyan Wu, Yougui Huang, Qiang Gao, Qingfu Zhang, Feilong Jiang, Maochun Hong*

Syntheses and characterization:

Synthesis of ligand 2,5-bis(4-pyridinylmethylthio)-1,3,4-thiadiazole (**L**): A solution of 2.63 g (16.00 mmol) 4-chloromethylpyridine hydrochloride and 1.20 g (8.00mmol) 2,5-dimercapto-1,3,4-thiadiazole in 40 mL methanol was stirred for 30 min, and 1.28 g (35 mmol) sodium hydroxide in 10 mL methanol was then added slowly and the mixture was refluxed vigorously for four hours. After concentrated to c.a. 10 mL, the solution was poured into 100 mL deionized water, and the result white precipitate was filtered and washed with diethyl ether. The yield of recrystallized material from chloroform/ petroleum ether (bp. 60–70 °C) was 1.63 g (c.a. 61.4%). ^{1}H NMR (CD_3CN, 25 °C): δ 8.52 (d, J = 6.0 Hz, 4H; H_a), 7.36 (d, J = 6.0 Hz, 4H; H_b), 4.44 (s, 4H; H_c). ESI-MS: m/z =333.4 (100%) [L+ H]. IR (KBr disc, cm^{-1}): 3038 (w), 2969 (w), 2922 (w), 1599 (s), 1556 (m), 1495 (m), 1416 (s), 1379 (s), 1334 (w), 1253 (w), 1220 (w), 1044 (s), 831 (m), 808 (m), 751 (m), 651 (w), 580 (w), 565 (w), 530 (w), 488 (s).

***CAUTION*!** Perchlorate salts of metal complexes are potentially explosive and should be handled with great care.

Synthesis of dinuclear silver(I) macrocycles solution (solution DSM·$(ClO_4)_2$; DSM= dinuclear silver(I) macrocycles): A solution of $AgClO_4$ (208 mg, 1mmol) in CH_3CN

(10 mL) was added dropwise to a stirred solution of **L** (332 mg, 1 mmol) in CH_3CN (10 mL). The mixed solution was stirred for further two hours and filtered. The solution **DSM**·$(ClO_4)_2$ can also be synthesized by solving complex **1, 2** or **2a** in CH_3CN. ^1H NMR (400MHz; CD_3CN, 25 °C): δ 8.48 (d, J = 6.0 Hz, 4H; H_a), 7.41 (d, J = 6.0 Hz, 4H; H_b), 4.44 (s, 4H; H_c).

Synthesis of complex 1: Slow evaporation of the solution **DSM**·$(ClO_4)_2$ (5ml) in the air afforded colorless block crystals. Yield: 117mg (ca. 87%). Anal. Calcd. for $C_{28}H_{24}N_8O_8S_6Cl_2Ag_2$: C, 31.15; H, 2.24; N, 10.38%. Found: C, 31.24; H, 2.17; N, 10.40%. ^1H NMR (400MHz; CD_3CN, 25 °C): δ 8.48 (d, J = 6.0 Hz, 4H; H_a), 7.41 (d, J = 6.0 Hz, 4H; H_b), 4.44 (s, 4H; H_c). IR (KBr disc, cm^{-1}): 3054 (w), 2968 (w), 2922 (w), 1603 (s), 1556 (w), 1496 (w), 1417 (s), 1379 (s), 1145 (s), 1110 (s), 1090 (s), 1004 (m), 836 (m), 814 (m), 751 (m), 627 (m), 492 (m).

Synthesis of complex 2: 5ml water was added to the solution **DSM**·$(ClO_4)_2$ (5ml) and the mixture was stirred for 2 hours. Slow evaporation of the mixture in the air afforded a large number of needles. Yield: 76.9 mg (ca. 51%). Anal. Calcd. for $C_{14}H_{19}N_4O_{7.5}S_3ClAg$: C, 27.89; H, 3.18; N, 9.29%. Found: C, 27.32; H, 3.69; N, 9.11%. IR (KBr disc, cm^{-1}): 3310 (m, br), 3054 (w), 2968 (w), 2922 (w), 1603 (s), 1556 (w), 1493 (w), 1416 (s), 1379 (s), 1145 (s), 1108 (s), 1090 (s), 1005 (m), 836 (m), 815 (m), 751 (m), 627 (m), 492 (m).

Synthesis of complex 2a: A 5ml solution **DSM**·$(ClO_4)_2$ was carefully layered on a H_2O/CH_3OH (5 ml, v/v=1:1) layer. Colorless crystals of **1** were grown after 48 hours. Yield: 91.6 mg (ca. 63%). Anal. Calcd. for $C_{15}H_{17}N_4O_{5.5}S_3ClAg$: C, 31.02; H, 2.95; N, 9.65%. Found: C, 31.17; H, 2.79; N, 9.66%. ^1H NMR (400MHz; CD_3CN, 25 °C): δ 8.48 (d, J = 6.0 Hz, 4H; H_a), 7.41 (d, J = 6.0 Hz, 4H; H_b), 4.44 (s, 4H; H_c), 3.30 (s, 3H; CH_3OH), 2.19 (s, 1H; H_2O). IR (KBr disc, cm^{-1}): 3310 (m, br), 3055 (w), 2968 (w), 2921 (w), 1603 (s), 1556 (w), 1495 (w), 1417 (s), 1379 (s), 1145 (s), 1108 (s), 1090 (s), 1005 (m), 836 (m), 815 (m), 751 (m), 627 (m), 492 (m).

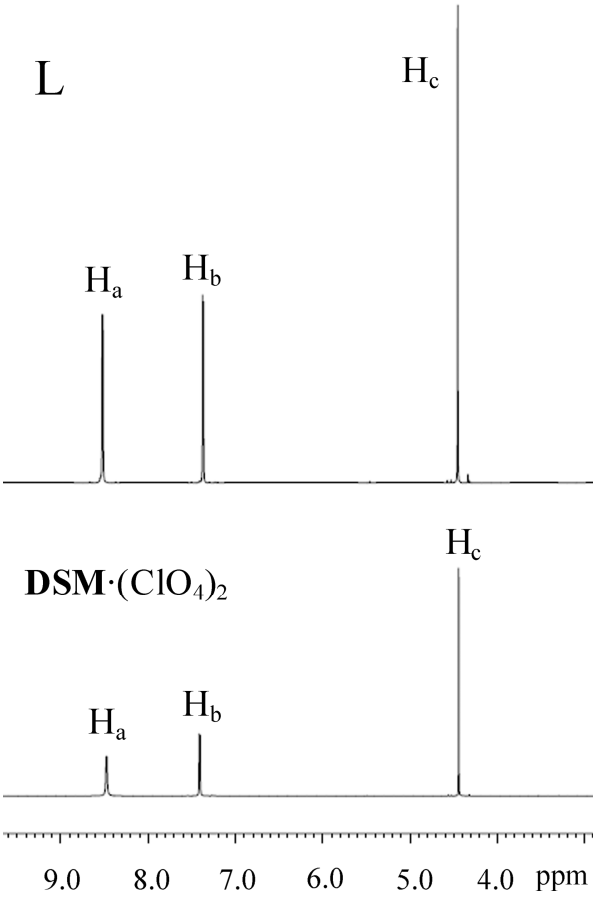

Figure S1 ^{1}H NMR spectra: ligand **L** and solution **DSM**·$(ClO_4)_2$ in CD_3CN.

^{1}H NMR spectra: Compared to the spectra of the "free" ligands (**L**), the proton signals of the complexes are only quite slightly shifted upfield (H_a) or downfield (H_b) (Chart 1). This observation is not in agreement with the normal expectation that the ligand proton resonances should be obviously shifted downfield upon coordination. The probable reason for the small shift is a result from two contrary effects: Primarily, an species with regular motif forms in the solution, and the protons on each pyridyl ring are shielded by the neighboring ring, resulting in an upfield shift owing to the ring current effect;[1] On the other hand, the protons on the pyridine rings will be shifted downfield as usual for the overall loss in electron density upon coordination.

References

(1) Chen, C.-L.; Tan, H.-Y.; Yao, J.-H.; Wan, Y.-Q.; Su, C.-Y. *Inorg. Chem.* **2005**, *44*, 8510.

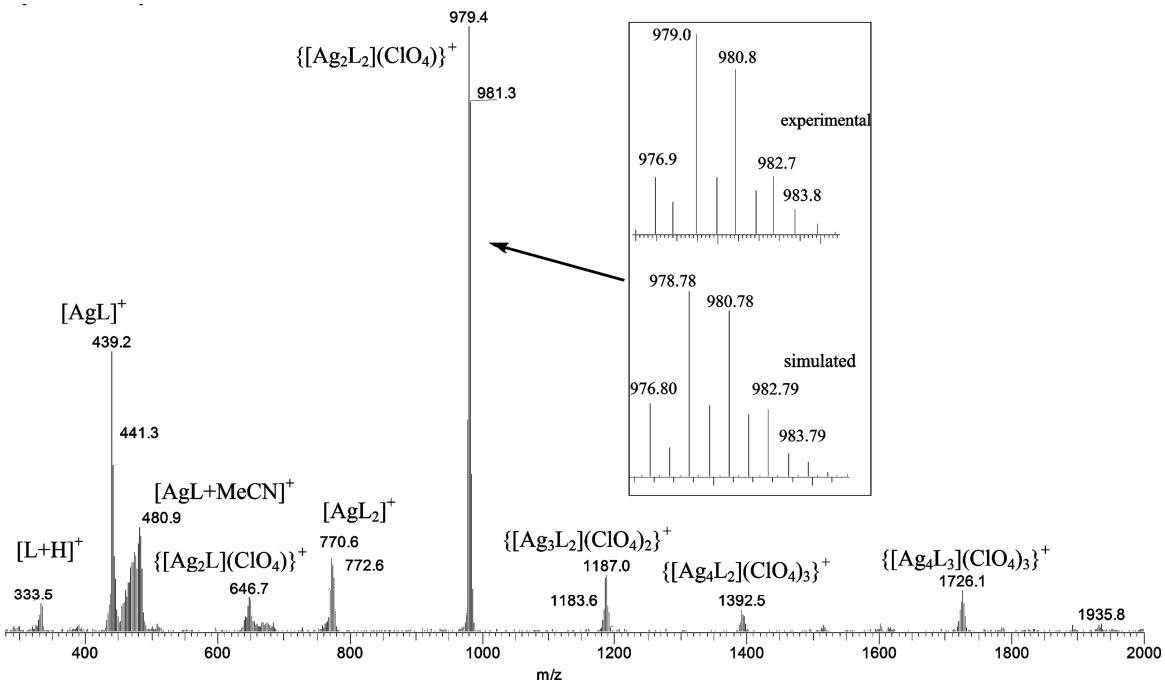

Figure S2 Partial ESI-MS spectrum of the solution **DSM**·$(ClO_4)_2$ (mixture of AgClO4 and **L** in a 1:1 ratio in CH_3CN).

ESI-MS spectrum: the ESI-MS spectrum exhibits a major peak at *m/z* 979 assignable to the disilver(I) metallacyclic $\{[Ag_2L_2](ClO_4)\}^+$ species. In addition, there are some relatively small peaks at *m/z* 334, 441, 481, 647, 773, 1187, 1394 and 1724, corresponding to $[L+H]^+$, $[AgL]^+$, $[AgL+MeCN]^+$, $\{[Ag_2L](ClO_4)\}^+$, $[AgL_2]^+$, $\{[Ag_3L_2](ClO_4)_2\}^+$, $\{[Ag_4L_2](ClO_4)_3\}^+$ and $\{[Ag_4L_3](ClO_4)_3\}^+$, respectively, which were verified by careful comparison of the isotopic patterns between the observed peaks and the theoretical simulations.

These results from the ^1H NMR spectra and ESI-MS indicate that the solution **DSM**·$(ClO_4)_2$ was expected to be in the equilibrium among some coordination species, but the dinuclear macrocyclic Ag_2L_2 species are dominant over others.

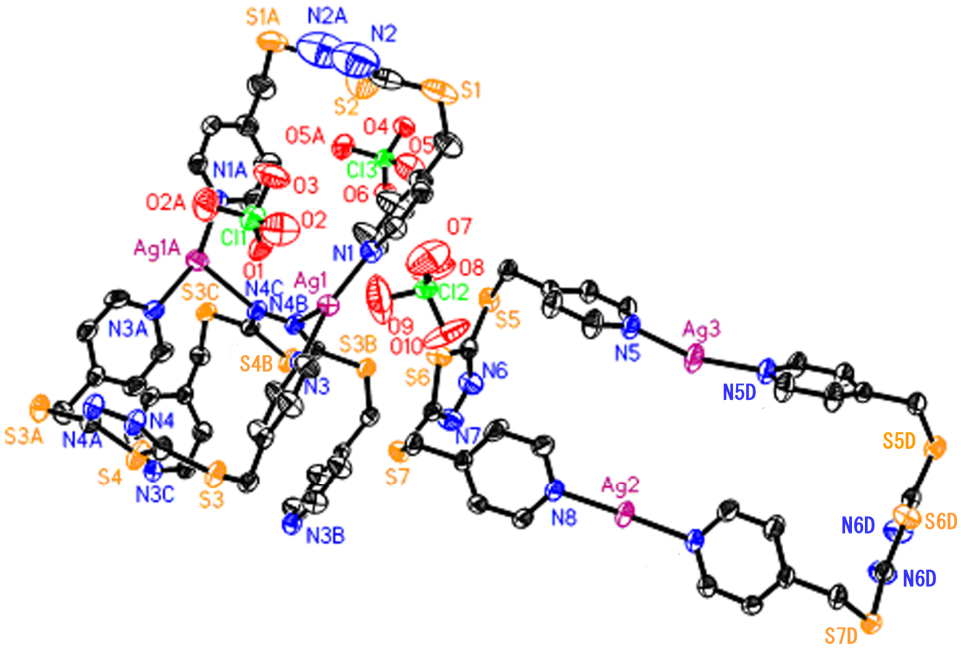

Figure S3 An ORTEP drawing of the silver (I) coordination environment in **1** with the thermal ellipsoids at 30% probability level. Symmetry codes: A –x, y, z; B x, -y, z-1/2; C -x, -y, z-1/2; D 1-x, y, z.

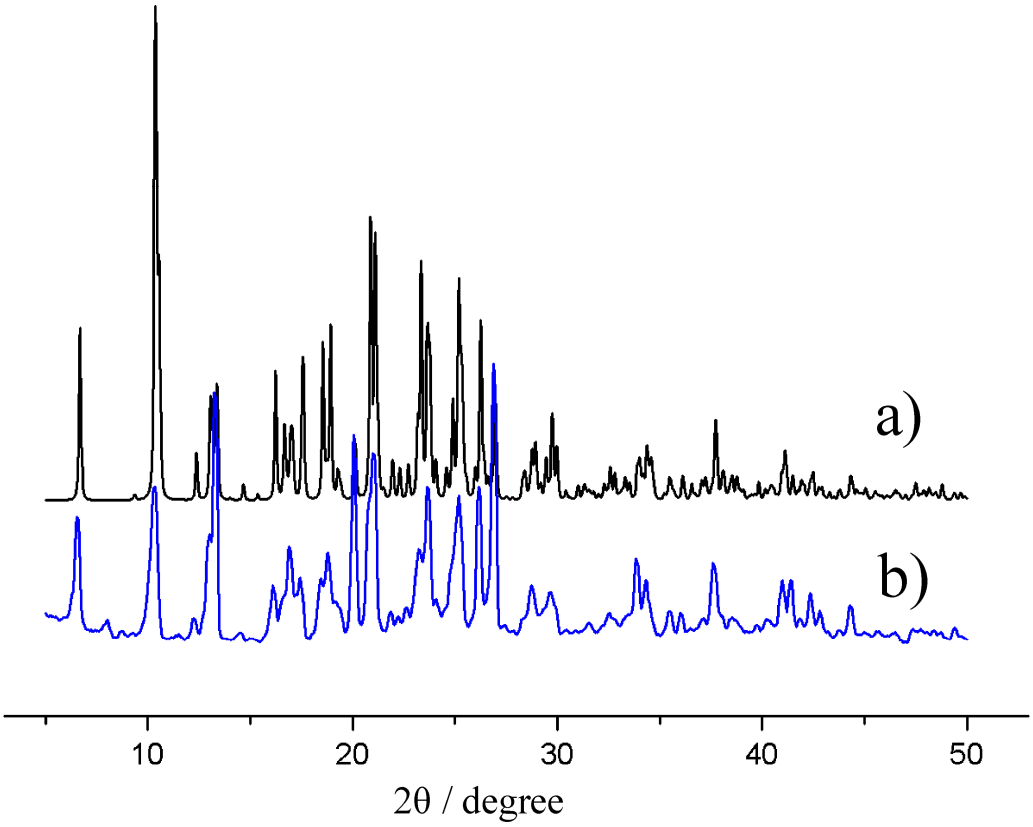

Figure S4 X-ray powder diffraction patterns of (a) **1** simulated, (b) **1** measured.

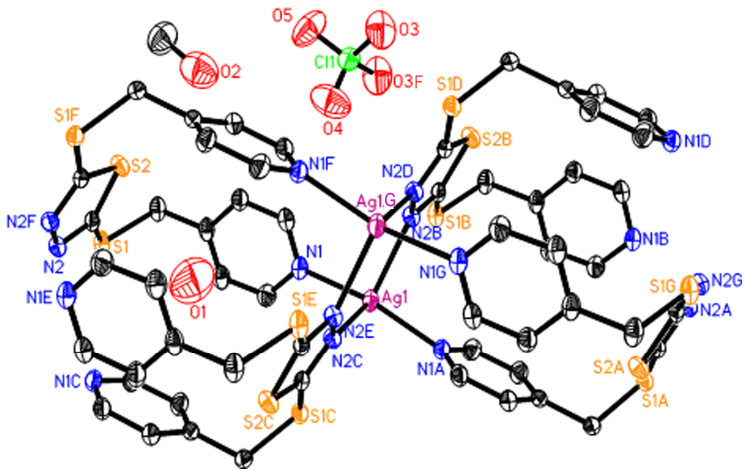

Figure S5 An ORTEP drawing of the silver (I) coordination environment in **2a** with the thermal ellipsoids at 30% probability level. Symmetry Code: A -x, y, -z; B x, y, z-1; C -x, y, 1-z; D x, -y, z-1; E -x, -y, 1-z; F x, -y, z; G -x, -y, -z.

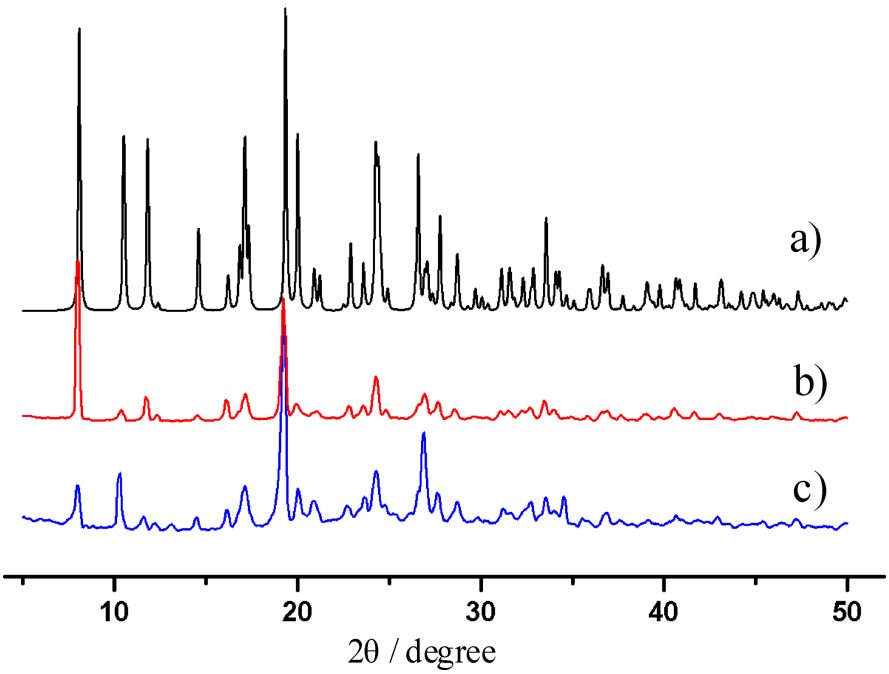

Figure S6 X-ray powder diffraction patterns of (a) **2a** simulated, (b) **2a** measured, (c) **2** simulated.

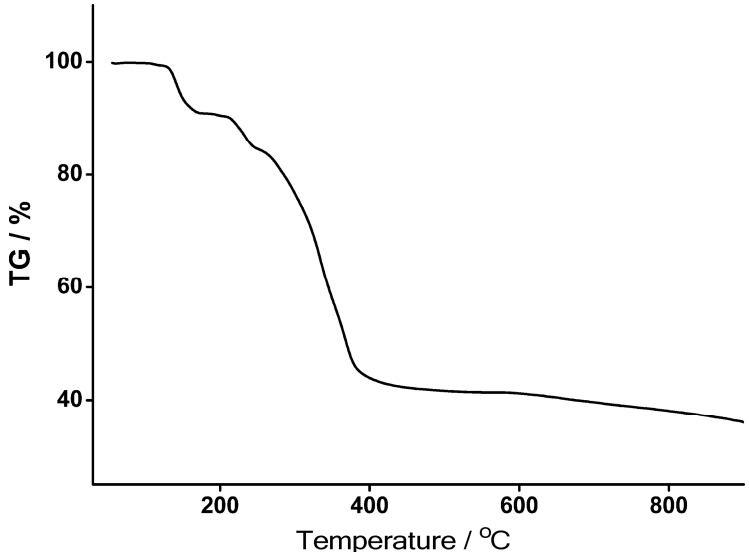

Figure S7 TGA curve of **2**.

TGA of **2** reveals two distinct weight loss regions. The first weight loss of 9.06 % from 112 to 209 °C is attributed to the release of the H_2O molecules (calcd = 8.97 % based on the formula $[Ag_2L_2]_n \cdot 2n(ClO_4) \cdot 7nH_2O$). The second weight loss in a very broad temperature range from 210 to 800 °C suggests the destruction of the framework with the loss of the organic component.

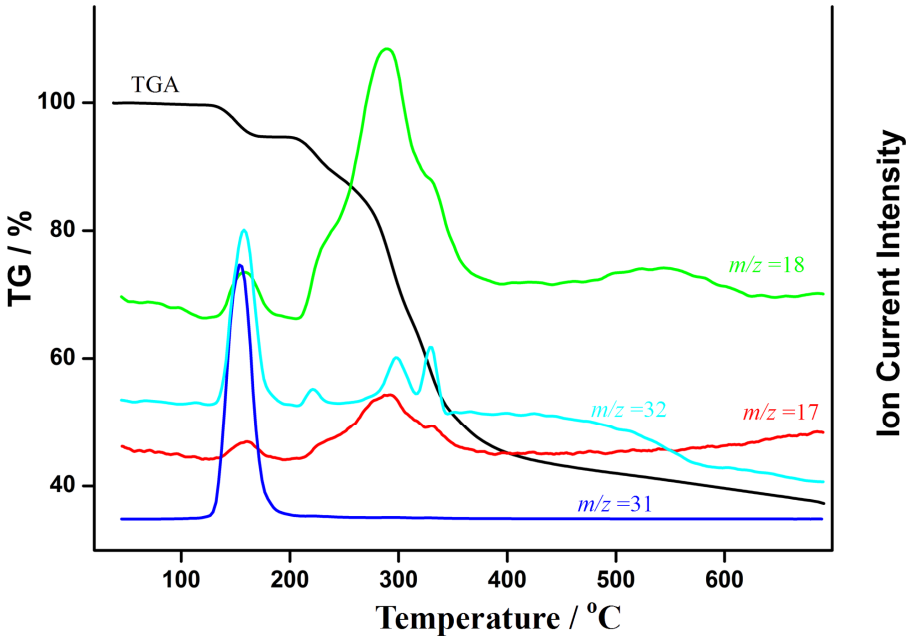

Figure S8 TG-MS analyses of complex **2a**.

TG-MS analyses: For further information on the release of the small guest molecules such as water and methanol molecules, TG-MS analyses were carried out on a thermogravimetry-mass spectrometry under a nitrogen atmosphere from 40 °C to 700 °C with a heating rate of 10 °C/min. The TGA of **2a** reveals two distinct weight loss regions. The first weight loss of 5.37% from 120 to 207 °C is attributed to the release of the MeOH molecules (calcd=5.52%). The second weight loss in a very broad temperature range from 210 to 700 °C suggests the destruction of the framework with the loss of the organic component and the trapped water molecules. These signals of *m/z* = 17, 18, 31 and 32 correspond to the ion current peaks of H_2O (*m/z* = 17, 18) and CH_3OH (*m/z* = 31, 32), respectively. Noticeably, the maximum of the signals involving H_2O molecules (*m/z* = 17, 18) appear at 288 °C, a temperature when the organic ligands has largely lost, and this result implies that the water molecule couldn't be released until the framework has collapsed, which no doubt confirms the water molecule's captivity in the aromatic cell.

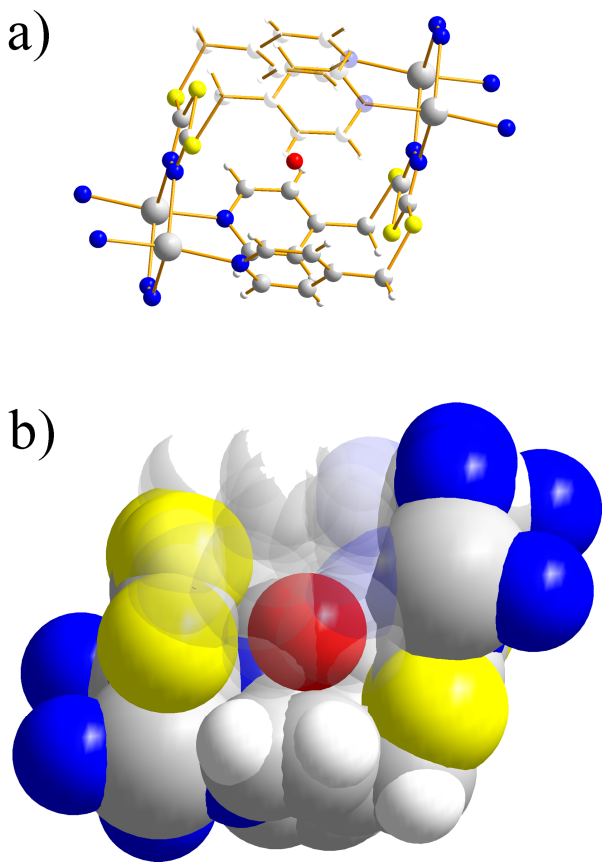

Figure S9 The water molecule captured in a hydrophobic aromatic cell in stick bond representation (a), and in space-filling representation (b).

Table S1. Selected bond lengths (Å) and angles (°) for all the complexes

1		**2a**	
Bond lengths (Å)		Bond lengths (Å)	
Ag1-N1	2.172 (4)	Ag1-N1	2.229 (3)
Ag1-N3	2.192 (4)	Ag1-N2^{ii}	2.472 (3)
Ag1-N4^{i}	2.594 (4)		
Ag2-N8	2.128 (4)		
Ag3-N5	2.129 (4)		
Bond angles (°)			
N1-Ag1-N3	161.06 (17)	N1-Ag1-N1^{i}	153.21 (16)
N1-Ag1-N4^{i}	98.79 (17)	N1-Ag1-N2^{ii}	99.08 (10)
N3-Ag1-N4^{i}	98.58 (16)	N1-Ag1-N2^{iii}	97.28 (10)
N8^{ii}-Ag2-N8	175.6 (3)	N1^{i}-Ag1-N2^{iii}	99.08 (10)
N5^{ii}-Ag3-N5	163.7 (3)	N2^{ii}-Ag1-N2^{iii}	104.25 (13)

Symmetry codes: **1** (i) x, -y, -1/2+z; (ii) 1-x, y, z. **2a**: (i) -x, y, -z; (ii) -x, y, 1-z; (iii) x, y, -1+z.